Protected 0-π states in SIsFS junctions for Josephson memory and logic

S. V. Bakurskiy,[1,2] N. V. Klenov,[3,1,2,4] I. I. Soloviev,[1,2] N. G. Pugach,[1,5] M. Yu. Kupriyanov,[1,2] and A. A. Golubov[2,6]

[1]Skobeltsyn Institute of Nuclear Physics, Lomonosov Moscow State University 1(2), Leninskie gory, Moscow 119234, Russian Federation
[2]Moscow Institute of Physics and Technology, Dolgoprudny, Moscow Region, 141700, Russian Federation
[3]Faculty of Physics, M.V. Lomonosov Moscow State University, 119992 Leninskie Gory, Moscow, Russia
[4]All-Russian Research Institute of Automatics n.a. N.L. Dukhov (VNIIA), 127055, Moscow, Russia
[5]National Research University Higher School of Economics, 101000, Moscow, Russia
[6]Faculty of Science and Technology and MESA+ Institute for Nanotechnology,
University of Twente, 7500 AE Enschede, The Netherlands
(Dated: August 23, 2018)

We study the peculiarities in current-phase relations (CPR) of the SIsFS junction in the region of 0 to π transition. These CPR consist of two independent branches corresponding to $0-$ and $\pi-$ states of the contact. We have found that depending on the transparency of the SIs tunnel barrier the decrease of the s-layer thickness leads to transformation of the CPR shape going in the two possible ways: either one of the branches exists only in discrete intervals of the phase difference φ or both branches are sinusoidal but differ in the magnitude of their critical currents. We demonstrate that the difference can be as large as 10% under maintaining superconductivity in the s layer. An applicability of these phenomena for memory and logic application is discussed.

Josephson junctions with ferromagnetic (F) layers in weak link region are considered as promising control elements in a superconducting memory compatible with RSFQ logic circuits[1–6]. The presence of two or more ferromagnetic layers in the weak-coupling region makes it possible to control the magnitude of the critical current J_C of these junctions by changing of mutual orientation of F films magnetization vectors[7–13]. It is necessary to mention that the large number of ferromagnetic layers in the weak-coupling area is accompanied by degradation of J_C by virtue of the larger number of interfaces in the structure, and owing to the strong suppression of superconducting correlations in each of the F layers.

In[14–19] it was shown that the required changes in J_C can also be ensured in SFS or SIsFS structures with single ferromagnetic layer. The remagnetization of the ferromagnetic layer in these junctions shifts the position of the maximum in Fraunhofer-like dependence of J_C on external magnetic field resulting in changing of J_C magnitude at zero field. This principle was extended in magnetic rotary valves[20,21] where the switching effect in J_C magnitude was achieved by changing the direction of the inplane F film magnetization.

It should be noted that magnetization reversal processes significantly increase the characteristic response time of the SFS control memory elements in comparison with the characteristic switching time of Josephson contacts in SFQ logic circuits. In order to overcome this drawback, it was suggested in[22] to use SIs-F/N-S contacts, where thin s-layer can be subdivided on superconducting domains with a phase shift of π. However, the implementation of the above mentioned proposals is a rather complicated technological task.

The promising concept of the Josephson memory with electrical control can be also realized using the phenomenon of the coexistense of the two metastable states in the vicinity of 0 - π transition[23,24]. For instance, these states can be achieved inside the region of the $0 - \pi$ transition of the junction with ferromagnetic layer[25–28] or in the junctions with two uncollinearly magnetized hard ferromagnets[29,30]. The conditions for the existence of metastable states essentially depend both on the material parameters of the contacts and on their geometry.

The purpose of this article is to propose the concept of the control element for memory based on our finding of noticable diiference between critical current in 0- and π- states in certain range of the s-layer thickness d_s in SIsFS junctions.

Figure 1 schematically shows the principle of operation of SIsFS structure in comparison with SFS or S-F/N-S devices. This figure demonstrates the evolution of the current-phase relation (CPR) $J_S(\varphi)$ and energy-phase relation (EPR) $E_S(\varphi)$ of SFS or S-F/N-S junctions and SIsFS structures in a vicinity of 0 to π transition, which occurs with increase of F layer thickness d_F.

For SFS junction the amplitude of the second harmonic in CPR is positive[27,28,31,32] at any transition point. The $0 - \pi$ transition is going through region of coexistence of the states with 0 and π phase differences (See Fig.1a). During the transition the depths of the corresponding minima in the $E_S(\varphi)$ relation are changing continuously until one of them disappears.

In the Josephson junctions with parallel $0-$ and $\pi-$ channels for the supercurrent flow inside a weak link region[33–37], e.g. S-F/N-S contacts, the amplitudes of the first harmonic in CPR in the channels have opposite signs and compensate each other. At the same time, the amplitudes of the second harmonic have negative signs in both channels. In this situation the transition from the initial 0 state to the final π state takes place via formation of so-called φ-state. With the increase of d_F (see Fig.1b) the minimum in $E_S(\varphi)$ located at $\varphi = 0$ splits into two minima located at some, $\pm\varphi(d_F)$, and this $\varphi(d_F)$ tends to $\varphi = \pi$ at the end of the transition.

In both $0 - \pi$ transitions presented in Fig.1a,b the $J_C(d_F)$ curves are V-shaped with a strong suppression of the critical current during the transitions. The metastable states in both structures generally have different barriers, which would be exceeded to switch device into resistive regime. It provides opportunity to read the state, although after that the state will
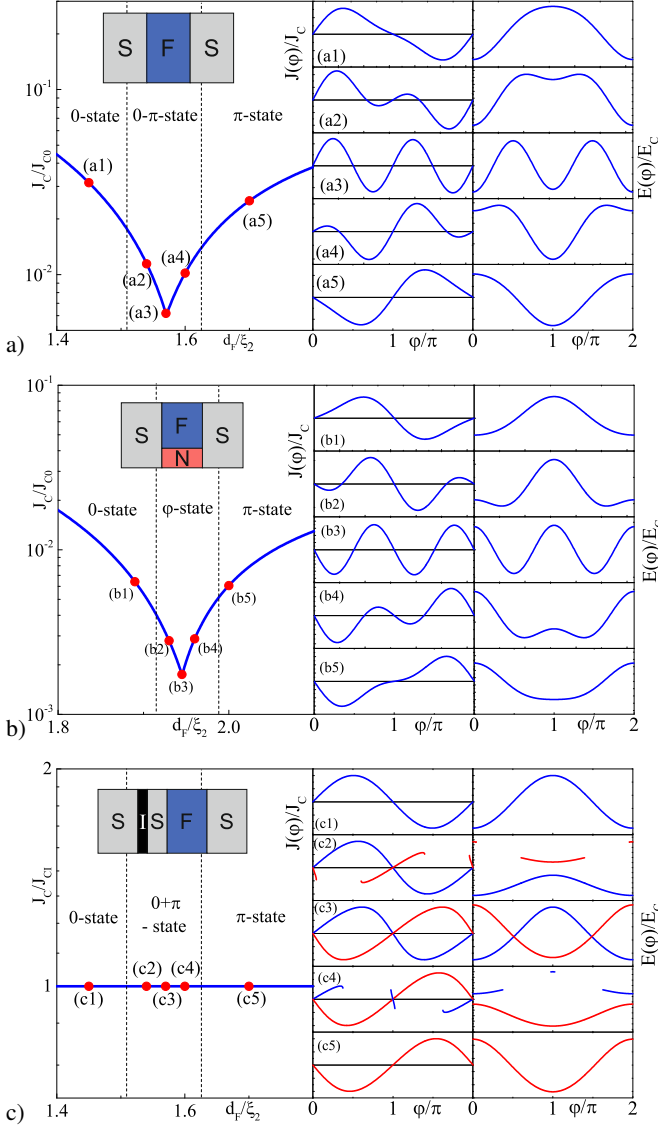
FIG. 1: Typical behaviour of a) SFS, b) S-F/N-S and c) SIsFS junctions characteristics in a vicinity of $0-\pi$ transition. Each block a)-c) includes 3 parts. The left one demonstrates dependence of the critical current J_C versus the ferromagnet layer thickness d_F. The middle row contains CPRs of the junctions at the certain d_F marked by the red dots (1)-(5) on the $J_C(d_F)$ dependence. Finally, the right row demonstrates EPRs at the same points.

be erased.

Contrary to that, in SIsFS devices[38–42] it is possible to realize the mode of operation in which magnitude of J_C of SIs part of the structure is smaller than the amplitude of the second harmonic in CPR of its sFS part. In this case (see Fig. 1c) $|J_C|$ is constant during the $0-\pi$ transition[40,42], although the current-phase relations undergo significant transformations and become multivalued. For relatively large layer thickness d_s there is the domain of SIsFS junction parameters providing its stay either in 0- or in π-ground state. The critical current is determined by SIs part of the junction and is exactly
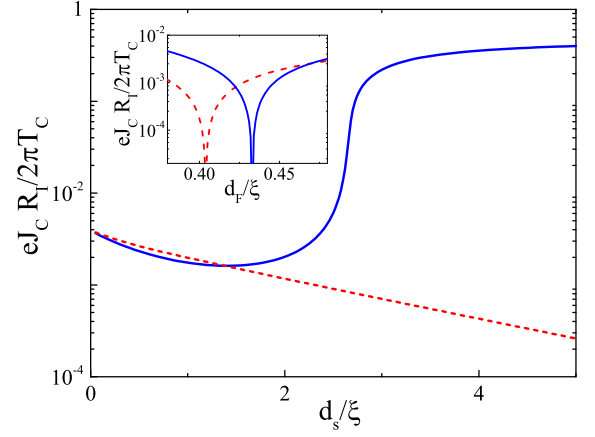
the same for the both states. In this domain a transition from one ground state to another is not possible by a continuous adiabatic variation of the phase φ and the states can be used for storage an information since the energy barrier separated them is higher than the energy of tunnel junction, thus protecting the system against accidental switching.

In order to model the SIsFS structure we suppose that the condition of a dirty limit is fulfilled for all metals and that effective electron-phonon coupling constant is zero in F layer. Under the above conditions the problem can be analyzed in the framework of the Usadel equations[43] with Kupriyanov-Lukichev boundary conditions[44] at the interfaces. The boundary-value problem was solved numerically using the algorithm developed in Ref.[42]. For simplicity we assume below that the resistivities ρ and coherence lengths $\xi = (D/2\pi T_C)^{1/2}$ of the SIsFS junction materials are the same. Here T_C is a critical temperature and D is a diffusion coefficient of superconducting material.

Based on our previous investigations[38,42] we have fixed the set of SIsFS junction parameters that ensure an occurrence of SIsFS contact in the vicinity of the $0-\pi$ transition at large s layer thickness $d_s = 5\xi$: $d_F = 0.46\xi$, $T = 0.26T_C$, exchange energy $H = 10\pi T_C$, suppression parameters of SF interface $\gamma_{BSF} = R_{BSF}\mathcal{A}/\xi\rho = 0.3$ and SIs interface $\gamma_{BI} = R_{BI}\mathcal{A}/\xi\rho = 5000$. Here R_B and $\mathcal{A}$ are the resistance and area of corresponding interface. With this choice of parameters the weakest link of the SIsFS structure is located at the tunnel barrier thus providing the coexistence of the two independent CPR branches (see example in the panel (c3) in Fig. 1c).

We start with calculation of the dependence of J_C magnitude on d_s, shown as a blue line in Fig. 2. It has a common form with a rapid drop of the critical current near the critical thickness $d_{sC} \approx 2.7\xi$. There are two independent processes going in the vicinity of this point. The first one is a shifting of the position and narrowing of the width of the $0-\pi$ transition during the decrease of the d_s, due to the change of the

FIG. 2: Magnitude of the critical current J_C of the SIsFS (solid blue) and the SInFS (dashed red) junctions versus thickness of the middle layer d_s calculated in the vicinity of $0-\pi$ transition at $d_F = 0.46\xi$ and $T = 0.26T_C$. Inset: Critical current J_C of the SIsFS (solid blue) and the SInFS (dashed red) junctions versus thickness of the F-layer d_F for s-layer thickness $d_s = 1\xi$ much smaller than d_{sC}.
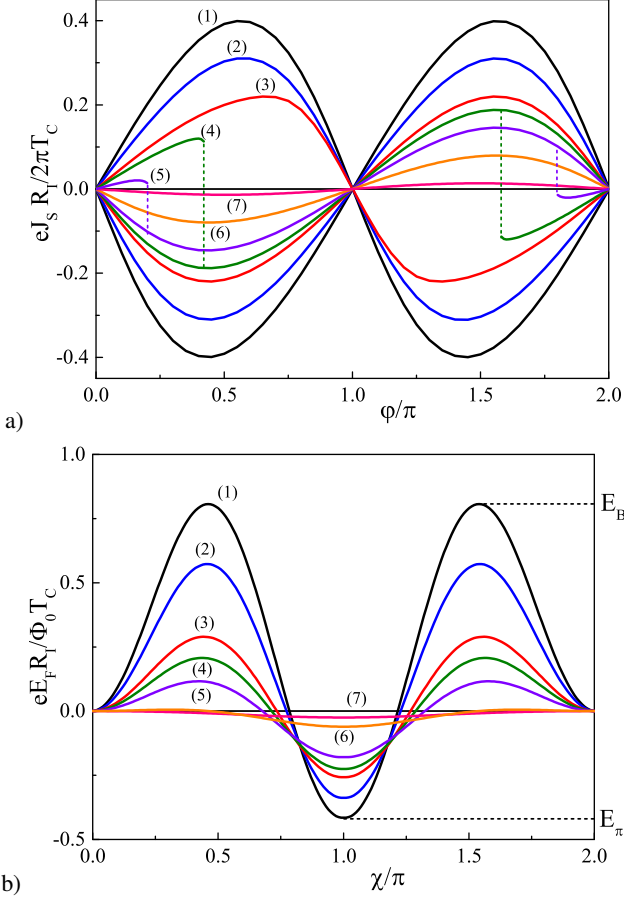
FIG. 3: The current-phase relation $J_S(\varphi)$ of the SIsFS junction (a) and the energy-phase relation $E_F(\chi)$ of the corresponding sFS junction (b) for the set of the different thicknesses of the s-layer d_s: (1) 5ξ, (2) 3.5ξ, (3) 3ξ, (4) 2.9ξ, (5) 2.8ξ, (6) 2.7ξ, (7) 2.6ξ. CPRs include 0 and π branches in the cases (1)-(5) and only π branch for (6)-(7). The calculations were done in the vicinity of $0-\pi$ transition at $d_F = 0.46\xi$, $T = 0.26T_C$ and $\gamma_B = 5000$.

effecting boundary condtions on F layer[16]. Inset in the Fig. 2 shows that transformation significantly differs from the process studied in the SInFS junction[45], since the residual pairing locks the phases of different Matsubara frequencies. This phenomenon leads to collapse of the 0-branch of the CPR at the d_s near the critical point.

The second phenomenon is the deviation of the pair amplitude in the thin s-electrodes for 0 and π states due to the different symmetry of the anomalous Green functions predicted and found experimentally in the sFs junctions with thin s-electrodes[46–48]. This effect can modify the critical currents of the tunnel SIs junction due to the changing of the s-layer properties in 0 and π states.

The relative impact of these processes on the SIsFS structure properties depends on the tunnel suppression parameter γ_{BI}. First, we consider the system at $\gamma_{BI} = 5000$, when the collapse of the 0-branch occurs.

Figure 3a demonstrates the evolution of the shape of $J_S(\varphi)$ dependence with decrease of the s layer thickness. It is

seen that the magnitudes of critical current of the both CPR branches are monothonically decreasing, while the shape of the curves transforms in different ways. The CPR of the π ground state remains sinusoidal at any d_s during the d_s decrease. The CPR at the some d_S the 0-branch becomes broken and disappears in the significant interval of phases. At $d_s \lesssim 2.7\xi$ it completely disappears and only the π ground state still exists. At the smaller $d_s \lesssim 2.5\xi$ critical current of the π-branch is strongly suppressed due to intensive suppression of the superconductivity in the s-layer by inverse proximity effect.

To understand the physics behind the $J_S(\varphi)$ transformations shown above it is convenient to use the so-called lump junction model[42] and consider the SIsFS junction as a series connection of SIs and sFS contacts with finite thickness d_s of the s electrode. The self-consistent problem for sFS junction was solved numerically with free boundary condition $d\Phi_s/dx = 0$ at the Is interface. The choice of the initial pair potential in iterative self-consistent calculation permits to find the magnitudes of Usadel functions Φ_s at Is interface for both 0 and π-states. Taking into account that the supercurrent flowing across the SIsFS structure is essentially small compare to s and S films depairing current, and that the d_s thicknesses of interest exceed 2.5ξ we can neglect a dependence of Φ_s magnitudes on phase differences χ and χ_1 across both sFS and SIs junctions, respectively. Under this assumption the critical current, I_C, and energy phase relation, $E_I(\chi_1)$, of SIs contact can be calculated using standard well-known expressions

$$\frac{eI_cR_I}{2\pi T_C} = \frac{T}{T_C}\mathrm{Re}\sum_{\omega>0}\frac{\Delta_0\Phi_s}{\sqrt{(\omega^2+\Delta_0^2)(\omega^2+\Phi_s^2)}}, \quad (1)$$

$$E_I(\chi_1) = E_{CI}(1-\cos(\chi_1)), \quad E_{CI} = \frac{\Phi_0 I_c}{2\pi}, \quad (2)$$

where R_I is the resistance of the tunnel barrier and Φ_0 is the magnetic flux quantum.

In the considered approximation the same quantities Φ_s can be used as boundary conditions of the first kind in calculating CPR $J_S(\chi)$ and EPR

$$E_F(\chi) = \frac{\Phi_0}{2\pi}\int_0^\chi J_S(\mu)d\mu, \quad (3)$$

of sFS contact (see Fig. 3b).

Figure 3b demonstrates that $E_F(\chi)$ dependence have the double-well form with the two minima at $\chi = \pi$ and $\chi = 0$ separated by a potential barrier E_B. The decrease of d_s is accompanied by suppression of the barrier height, $E_B(d_s)$. At $d_s \lesssim 2.7\xi$ the potential barrier completely disappears and the sFS contact stays only in the π ground state. The depth of the potential well for the π-state E_π also decreases rapidly with further decrease of d_s.

We summarize the dependence of the characteristical energies E_B (dashed black), $E_B - E_\pi$ (dash-dotted green) and E_{CI} versus thickness d_s in Fig. 4. The energy of tunnel junction E_{CI} is calculated in the frame of lumped junction model independently for 0- (solid red) and π- (short-dashed blue) states of sFS-electrode. It is seen, that they practically coincide with
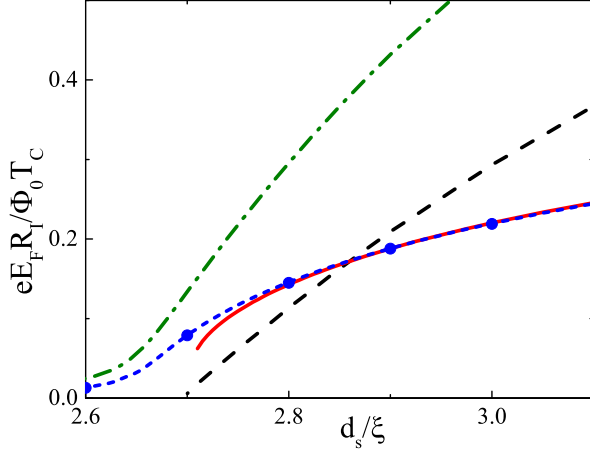
FIG. 4: The characteristical energies of the SIs and sFS junctions: barrier heights in sFS junction E_B (dashed black) and $E_B - E_\pi$ (dash-dotted green) and the energy of SIs junction E_{CI} in the 0- (solid red) and π- (short-dashed blue) states versus the thickness of s layer d_s. The blue dots mark the energies calculated from the CPR of SIsFS junction demonstrated on Fig. 3a.

FIG. 5: a) The 0− (solid red) and π− (dashed blue) branches of the CPR $J_S(\varphi)$ of the SIsFS junction with thin s-layer $d_s = 2.72\xi$ and strong $\gamma_B = 5 \cdot 10^7$.

each other for $d_s > 2.8\xi$. The blue dots mark the critical energies of the SIsFS junction shown in the Fig. 3. They correllate well with the results obtained in lumped junction model thus demonstrating the accuracy of our approach.

It follows from Fig. 4, that in the wide range of d_s the tunnel energy $E_{CI} \ll E_B, E_B - E_\pi$. These conditions provide existence of two independent continuous branches of CPR in SIsFS junction for the both 0- and π-states as it is seen in Fig. 3a. With the decrease of d_s, the barrier height E_B is suppressed more rapidly than E_{CI}. At $d_s \approx 2.8\xi$ the energies E_B and E_{CI} become comparable and adiabatic increase of φ leads to escape of the system from the metastable to the ground state resulting in discontinues jump in $J_S(\varphi)$. Finally, at the critical thickness $d_s \approx 2.7\xi$ the barrier completely vanishes, leading to dissappearence of the 0-branch. At the same time, the barrier for the π-state significantly exceeds E_{CI} in the whole considered interval.

In the region near the critical thickness $d_s \approx 2.7\xi$ the energies of tunnel SIs junction corresponding to 0- (red) and π- (blue) states deviate. The absolute values of Green function Φ_s and pair potential Δ on the tunnel SIs interface are different for 0 and π states. In contrast to Ref.[46–48], we find that π-state has a larger value of Δ and larger critical current.

The difference between 0 and π-states provides significant influence on the CPR and critical current of SIsFS structure at the larger values of tunnel layer parameter γ_{BI}. Increase of γ_{BI} doesn't modify the barrier height $E_B(d_s)$ of the SFs-junction, but proportionally decreases the $E_{CI}(d_s)$, shifting the cross-point between them to the critical thickness d_{sC}.

For instance, for the value of suppression parameter $\gamma_{BI} = 5 \cdot 10^7$ direct calculations of SIsFS structure show that the both branches of CPR have sinusoidal shape and are defined for all phases φ even at $d_s = 2.72\xi$ (See Fig. 5). It is important to note that for this particular case the critical currents J_{C0} and
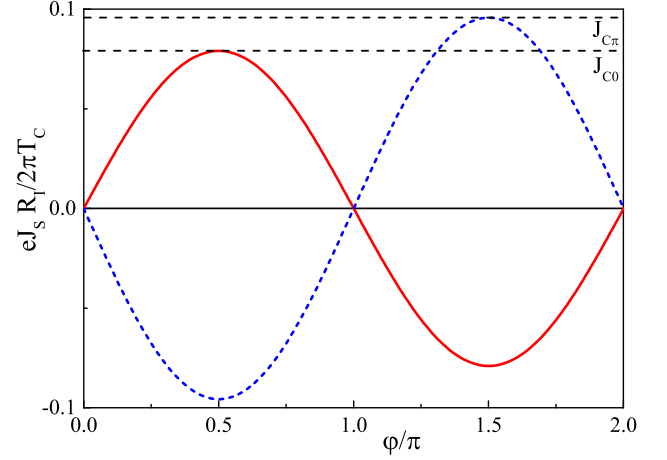
$J_{C\pi}$ of 0- and π- CPR branches are different from each other and this difference $(J_{C\pi} - J_{C0})/J_{C0}$ is of the order 10%.

The ability of the structure to be in one of two states differing in their critical currents can find applications in superconductor logic and memory devices. Information on the state of the SIsFS structure can be obtained by setting a current pulse, with an amplitude, J in the range $J_{C0} < J < J_{C\pi}$. It is determined by the absence (π− state) or by the generation (0− state) of the corresponding voltage pulse. Reading the state of the element will be non-destructive, if the incoming energy is insufficient to open the channel of tunneling through the energy barrier separating the 0− and π− states. The recording is possible with current pulses, which have an amplitude exceeding the critical current of sFS junction and switch the system from 0 to π- state and back[24].

The drawback of this concept is in strong limitation on thickness of both the superconducting and ferromagnetic layers and the smallness of the critical currents. The thickness of the s layer should be close to its critical value with an accuracy of the order of $0.1\xi \approx 1$ nm, while the thickness of the ferromagnet should ensure the occurence of that $0 - \pi$ transition. On the other hand, recent experiments[27,28] have demonstrated the feasibility of this task.

The advantages of the proposed SIsFS element compared to spin-valves[10–13] or single flux quantum (SFQ) devices[49,50] are obvious. The proposed control memory element stores an information only in the phase difference across the junction in the steady state. Thus, it makes use of its own intrinsic properties to store an information, so that there is neither need in remagnetization of the F layers, nor in holding a flux quantum.

In this sense, the bistable SIsFS device may serve as a truly Josephson memory device, which permits the reduction of size of the auxiliary circuits or even provide an alternative to the SFQ concept of superconducting electronics.

---

1. M. Eschrig, Reports on Progress in Physics, **78**, 104501 (2015).

2. J. Linder, J. W. A. Robinson, Nature Physics, **11**, 307 (2015).

3. M. G. Blamire, J. W. A. Robinson, Journ. Phys. Cond. Mat., **26**, 453201 (2014).

4. J. W. Lu, E. Chen, M. Kabir, V. R. Stan, S. A. Wolf, Int. Materials Reviews **61**, 456 (2016).

5. O. A. Mukhanov, Digital Processing, Superconductor Digital Electronics. In Applied Superconductivity: Hand-book on Devices and Applications; Seidel, P., Ed., Wiley-VCH Verlag GmbH & Co. KGaA: Weinheim, Germany (2015).

6. I. I. Soloviev, N. V. Klenov, S. V. Bakurskiy, M. Yu Kupriyanov, A. L. Gudkov, and A. S. Sidorenko, Beilstein Journal of Nanotechnology, **8**, 2689 (2017).

7. A. A. Golubov, M. Yu. Kupriyanov, E. Il'ichev, Rev. Mod. Phys. **76**, 411 (2004).

8. A. I. Buzdin, Rev. Mod. Phys. **77**, 935 (2005).

9. F. S. Bergeret, A. F. Volkov, K. B. Efetov, Rev. Mod. Phys. **77**, 1321 (2005).

10. C. Bell, G. Burnell, C. W. Leung, E. J. Tarte, D.-J. Kang and M. G. Blamire, Appl. Phys. Lett., **84**, 1153 (2004).

11. M. A. E. Qader, R. K. Singh, Sarah N. Galvin, L. Yu, J. M. Rowell, and N. Newman, Appl. Phys. Lett., **104**, 022602 (2014).

12. B.Baek, W.H.Rippard, S.P.Benz, S.E.Russek, and P.D. Dresselhaus, Nature Communications, **5**, 3888 (2014).

13. B. M. Niedzielski, T. J. Bertus, J. A. Glick, R. Loloee, W. P. Pratt, Jr., and N. O. Birge Phys. Rev. B 97, 024517 (2018).

14. V. V. Bol'ginov, V. S. Stolyarov, D. S. Sobanin, A. L. Karpovich, and V. V. Ryazanov, Pis'ma v ZhETF **95**, 408 (2012) [JETP Lett. **95** 366 (2012)].

15. T. I. Larkin, V. V. Bol'ginov, V. S. Stolyarov, V. V. Ryazanov, I. V. Vernik, S. K. Tolpygo, and O. A. Mukhanov, Appl. Phys. Lett. **100**, 222601 (2012).

16. I. V. Vernik, V. V. Bol'ginov, S. V. Bakurskiy, A. A. Golubov, M. Yu. Kupriyanov, V. V. Ryazanov and O. A. Mukhanov, IEEE Tran. Appl. Supercond., **23**, 1701208 (2013).

17. S. V. Bakurskiy, N. V. Klenov, I. I. Soloviev, V. V. Bol'ginov, V. V. Ryazanov, I. I. Vernik, O. A. Mukhanov, M. Yu. Kupriyanov, and A. A. Golubov, Appl. Phys. Lett. **102**, 192603 (2013).

18. R. Caruso, D. Massarotti, A. Miano, V. V. Bolginov, A. Ben Hamida, L. N. Karelina, G. Campagnano, I. V. Vernik, F. Tafuri, V. V. Ryazanov, O. A. Mukhanov, and G. P. Pepe, IEEE Trans. Appl. Supercond., **28**, 7, 1800606, (2018).

19. R. Caruso, D. Massarotti, V. V. Bolginov, A. Ben Hamida, L. N. Karelina, A. Miano, I. V. Vernik, F. Tafuri, V. V. Ryazanov, O. A. Mukhanov, G. P. Pepe, Journ. Appl. Phys., **123**, 133901 (2018).

20. I. I. Soloviev, N. V. Klenov, S. V. Bakurskiy, V. V. Bol'ginov, V. V. Ryazanov, M. Yu Kupriyanov, and A. A. Golubov, Appl. Phys. Lett., **105**, 242601 (2014).

21. I. I. Soloviev, N. V. Klenov, S. V. Bakursky, M. Yu Kupriyanov, and A. A. Golubov, JETP Letters, **101**, 240 (2015).

22. S. V. Bakurskiy, N. V. Klenov, I. I. Soloviev, M. Yu Kupriyanov, and A. A. Golubov, Appl. Phys. Lett., **108**, 042602 (2016).

23. E. Goldobin, H. Sickinger, M. Weides, N. Ruppelt, H. Kohlstedt, R. Kleiner, D. Koelle, Appl. Phys. Lett. **102** (24), 242602 (2013).

24. R. Menditto, H. Sickinger, M. Weides, H. Kohlstedt, M. Zonda, T. Novotny, D. Koelle, R. Kleiner, E. Goldobin, Physical Review B **93** (17), 174506 (2016).

25. J. J. A. Baselmans, T. T. Heikkila, B. J. van Wees, and T. M. Klapwijk, Phys. Rev. Lett. **89**, 207002 (2002).

26. S. M. Frolov, D. J. Van Harlingen, V. A. Oboznov, V. V. Bolginov, and V. V. Ryazanov, Phys. Rev. B **70**, 144505 (2004).

27. B. Baek, M. Schneider, M. R. Pufall, W. H. Rippard, IEEE Tran. Appl. Supercond., **28**, 7, 1800705 (2018).

28. M.J.A. Stoutimore, A.N. Rossolenko, V.V. Bolginov, V.A. Oboznov, A.Y. Rusanov, N. Pugach, S.M. Frolov, V.V. Ryazanov, D.J. Van Harlingen, arXiv:1805.12546 (2018).

29. L. Trifunovic, Z. Popovic, and Z. Radovic Phys. Rev. B **84**, 064511 (2011).

30. C. Richard, M. Houzet, J. S. Meyer, Phys. Rev. Lett., **110** (21), 217004 (2013).

31. A. Buzdin Phys. Rev. B 72, 100501(R) (2005).

32. F. Konschelle, J. Cayssol, A.I. Buzdin, Phys. Rev. B **78**, 134505 (2008).

33. A. Buzdin and A. E. Koshelev, Phys. Rev. B **67**, 220504(R) (2003).

34. N. G. Pugach, E. Goldobin, R. Kleiner, D. Koelle, Physical Review B, **81**(10), 104513 (2010).

35. E. Goldobin, D. Koelle, R. Kleiner, and R.G. Mints, Phys. Rev. Lett, **107**, 227001 (2011).

36. S. V. Bakurskiy, N. V. Klenov, T. Yu. Karminskaya, M. Yu. Kupriyanov, and A. A. Golubov, Supercond. Sci. Technol. **26**, 015005 (2013).

37. H. Sickinger, A. Lipman, M. Weides, R. G. Mints, H. Kohlstedt, D. Koelle, R. Kleiner, E. Goldobin, Phys. Rev. Lett. **109**, 107002 (2012).

38. S. V. Bakurskiy, N. V. Klenov, I. I. Soloviev, M. Yu. Kupriyanov, and A. A. Golubov, Phys. Rev. B **88**, 144519 (2013).

39. I. P. Nevirkovets, O. Chernyashevskyy, G. V. Prokopenko, O. A. Mukhanov, J. B. Ketterson, IEEE Trans. on Appl. Supercon. **24**, 4, (2014).

40. N. Ruppelt, H. Sickinger, R. Menditto, E. Goldobin, D. Koelle, R. Kleiner, O. Vavra, H. Kohlstedt, Appl. Phys. Lett., **106**, 022602 (2015).

41. S. Shafranjuk, I. P. Nevirkovets, O. A. Mukhanov, and J. B. Ketterson, Phys. Rev. Applied **6**, 024018, (2016).

42. S. V. Bakurskiy, V. I. Filippov, V. I. Ruzhickiy, N. V. Klenov, I. I. Soloviev, M. Yu Kupriyanov, and A. A. Golubov, Phys. Rev. B **95**, 094522 (2017).

43. K. D. Usadel, Phys. Rev. Lett. **25**, 507 (1970).

44. M. Yu. Kuprianov and V. F. Lukichev, Zh. Eksp. Teor. Fiz. **94**, 139 (1988) [Sov. Phys. JETP **67**, 1163 (1988)].

45. D. M. Heim, N. G. Pugach, M. Yu. Kupriyanov, E. Goldobin, D. Koelle, R. Kleiner, N. Ruppelt, M. Weides, H. Kohlstedt, New J. Phys. **17** 113022 (2015).

46. N. Pompeo, K. Torokhtii, C. Cirillo, A. V. Samokhvalov, E. A. Ilyina, C. Attanasio, A. I. Buzdin, and E. Silva Phys. Rev. B **90**, 064510 (2014).

47. A. V. Samokhvalov and A. I. Buzdin, Phys. Rev. B **92**, 054511 (2015).

48. S. N. Vdovichev, Yu. N. Nozdrin, E. E. Pestov, P. A. Yunin, A. V. Samokhvalov, JETP Lett. **104**, 329 (2016).

49. T. Golod, A. Iovan, V. M. Krasnov, Nature communications **6**, 8628 (2015).

50. A. Murphy, D. Averin, A. Bezryadin, New J. Phys. **19** (6), 063015 (2017).